ORIGINAL SCIENTIFIC PAPER OPEN ACCESS

Wild horse optimizer: an application to identify damage for space truss structures

Hoang Lan Ton-That[1*]

[1] University of Architecture, Department of Civil Engineering, Ho Chi Minh City, Vietnam

ARTICLE INFO

[*] **Correspondence:** lan.tonthathoang@uah.edu.vn

DOI: 10.5937/engtoday2600008T

UDC: 621(497.11) **ISSN:** 2812 – 9474

Article history: Received 14 January 2026; Revised 26 February 2026; Accepted 2 March 2026

ABSTRACT

These days, optimization algorithms are widely used to tackle issues in a variety of scientific domains. The natural behavior of an agent - which could be a physical or chemical agent, a human, an animal, or a plant - is typically the source of inspiration for optimization algorithms. Animal behavior served as the inspiration for the majority of algorithms that have been proposed in the past ten years. The wild horse optimizer (WHO), an optimizer algorithm inspired by the social behavior of wild horses, is used in this paper to identify damage to space truss constructions. As we know, a stallion and a number of mares and foals typically make up a group of horses. Horses engage in a variety of activities, including grazing, pursuing, leading, dominating, and mating. The decency of horses is an intriguing trait that sets them apart from other animals. The offspring of the horse leave the group before they reach adolescence and join other groups due to horse descent behavior. The purpose of this departure is to stop the father from mating with the daughter or siblings. The key to WHO was established. In addition, based on finite element analysis to determine the natural frequencies and mode shapes of these space truss structures for the goal of establishing the objective function, the final results demonstrate a very good reaction to the suggested tasks.

KEYWORDS

Space truss structure, Identify damage, Finite element analysis, Natural frequency, Mode shape, Wild horse optimizer.

1. INTRODUCTION

The rapid advancement of science and technology has led to the widespread use of artificial intelligence techniques in contemporary society. Because optimization can choose the optimum answer from a range of choices, it is an essential part of artificial intelligence. Three basic components are typically included in an optimization problem: the objective function(s), design variables, and constraints that require the optimization method to reach the global result. Because of their many advantages, including population-based mechanisms with multiple candidate solutions, ease of implementation, high flexibility, lack of gradient information, and black-box processes with only inputs and outputs, metaheuristic algorithms—a stochastic optimization technique inspired by natural behaviors-have become more and more popular in the optimization fields. For optimization issues like those in mechanical design and civil engineering, metaheuristic algorithms are therefore highly suitable. Particle Swarm Optimization (PSO) [1], Genetic Algorithm (GA) [2], Gravitational Search Algorithm (GSA) [3], Salp Swarm Algorithm (SSA) [4], Artificial Bee Colony (ABC) [5], Gray Wolf Optimizer (GWO) [6], Wild Horse Optimizer (WHO) [7], Evolution Strategies [8], Water Flow Optimizer (WFO) [9], Sine Cosine Algorithm (SCA) [10], Black Widow Optimization Algorithm (BWOA) [11], Teaching–Learning-Based Optimization (TLBO) [12], Chaos Game Optimization (CGO) [13], and many other metaheuristic algorithms have already been developed by researchers and engineers. Even while metaheuristics range in their performance and sources of inspiration, striking a balance between exploration and exploitation remains a common problem. Exploration refers to the search agents' ability to search globally, whereas exploitation is related to their ability to search locally. A metaheuristic algorithm may experience local stagnation if it is unable to strike a balance between exploration and exploitation. It is important to remember that because all metaheuristic algorithms rely on stochastic search, they cannot guarantee global convergence for every optimization problem. Researchers can determine the advantages and disadvantages of the suggested metaheuristic algorithm as well as any potential drawbacks by carrying out thorough experiments and algorithm comparisons. This is crucial when creating new metaheuristic algorithms for optimization.

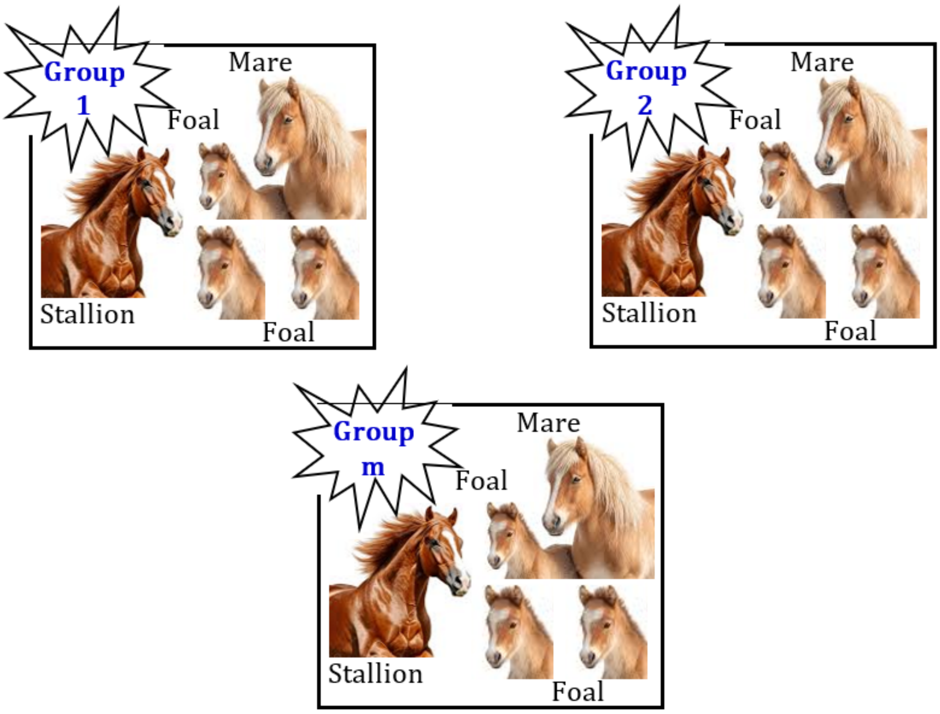

Figure 1: Horse groups based on the initial population

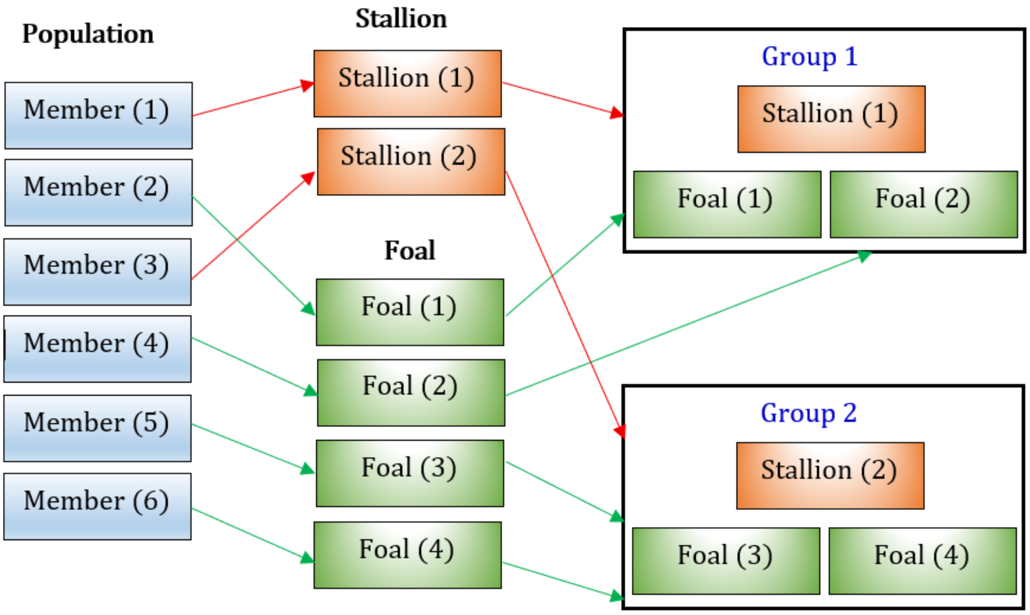

Figure 2: The creation of horse groups

In this study, damage to space truss structures is predicted using the Wild Horse Optimization (WHO), which was inspired by the behavior of horse herds in the wild (Figures 1 and 2). Some formulas for calculating the natural frequencies as well as mode shapes of a structure using the traditional finite element method should be read, such as those included in the documents [14, 15].

This paper is divided into the following sections: Section 2 presents a brief theory. Section 3 gives the results, and the final section offers some remarks.

2. THE BRIEF RECALL ON WHO

Horses are classified into two social groups: territorial and non-territorial. The authors of WHO [7] concentrated on the non-territorial group. They provided the following pseudo-code for the WHO algorithm:

Step 1: Initialize the first population of horses randomly

Step 2: Enter the required parameters PC and PS

Step 3: Calculate the fitness of horses

Step 4: Form groups of foals and choose stallions

Step 5: Find the best horse as the optimum

Step 6: While the end criterion is not satisfied, calculate TDR

$$TDR = 1 - iter \,/\, \max iter \tag{1}$$

Step 7: For the number of stallions, calculate Z, an adaptive mechanism.

Step 8: With sub-loop, for the number of foals of any group.

If *rand > PC, update the position of the foal*

$$\bar{X}_{i,G}^{j} = 2Z\cos(2\pi RZ)\times\left(Stallion^{j} - X_{i,G}^{j}\right) + Stallion^{j} \tag{2}$$

with G is the number of horse groups.

Else, *update the position of the foal*

$$X_{G,k}^{p} = Crossover\left(X_{G,i}^{q}, X_{G,j}^{z}\right) \tag{3}$$

with details stated in document [7].

End

Step 9:

If *rand > 0.5, update the position of stallion* ($Stallion_{G_i}^{*}$)

$$Stallion_{G_i}^{*} = 2Z\cos(2\pi RZ)\times\left(WH - Stallion_{G_i}\right) + WH \tag{4}$$

Else, *update the position of stallion* ($Stallion_{G_i}^{*}$)

$$Stallion_{G_i}^{*} = 2Z\cos(2\pi RZ)\times\left(WH - Stallion_{G_i}\right) - WH \tag{5}$$

in which WH is the position of the water hole.

End

Step 10:

If *cost(* $Stallion_{G_i}^{*}$ *) < cost(Stallion)*

$$Stallion = Stallion_{G_i}^{*} \tag{6}$$

End

Step 11: Sort foals of group by cost. Select foal with minimum cost.

If *cost(Foal) < cost(Stallion), exchange foal and stallion position*

$$Stallion_{G_i} = \begin{cases} X_{G,i}, \ \ if \ \ \cos t\left(X_{G,i}\right) < \cos t\left(Stallion_{G_i}\right) \\ Stallion_{G_i}, \ if \ \ \cos t\left(X_{G,i}\right) > \cos t\left(Stallion_{G_i}\right) \end{cases} \tag{7}$$

End

Step 12: Update optimum and finish.

It should be noted that further parameters for the aforementioned formulas can be found in the pertinent literature on the WHO's founding by [7]. Figure 3 displays the qualitative analysis results of the WHO approach in resolving a number of typical optimization problems. Details and comprehensive information on these functions are described in [4-6].

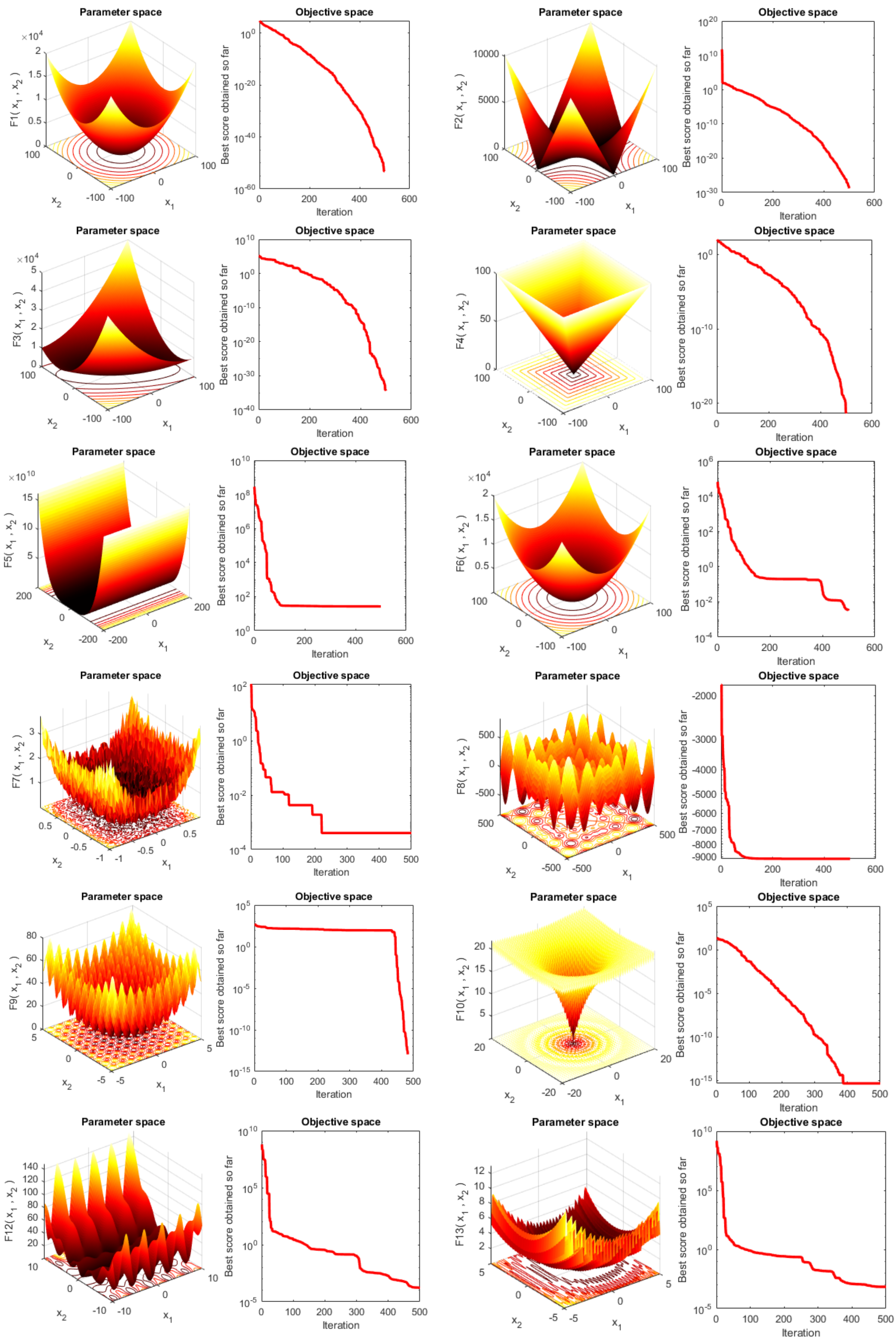

Figure 3: Qualitative analysis related to WHO

3. RESULTS

Two space truss configurations with 25 and 72 bars are examined in this section, as shown in Figures 4 and 5 and Tables 1 through 3.

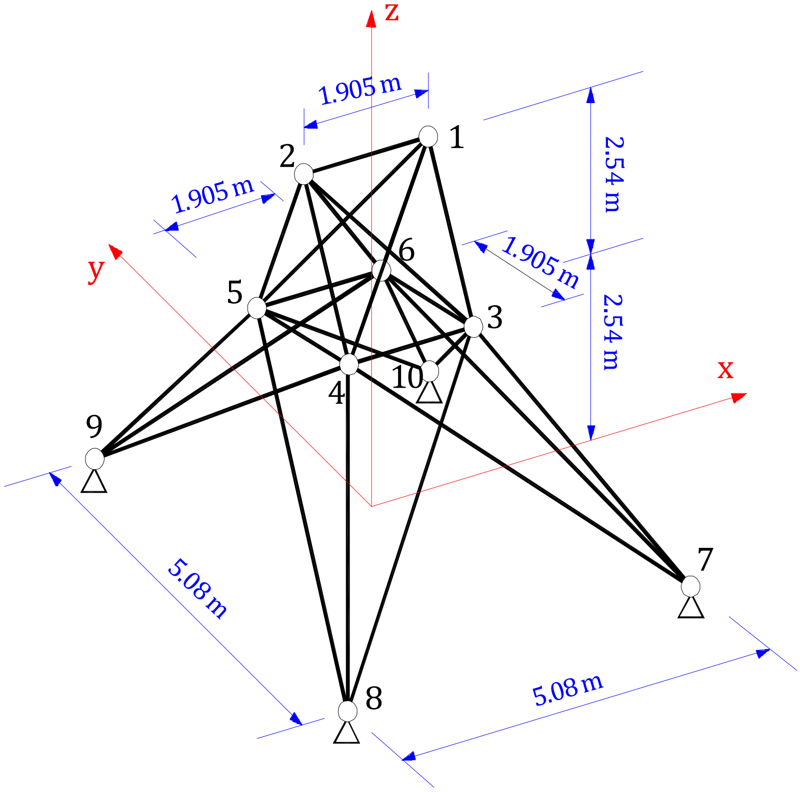

Figure 4: 25-bar truss structure

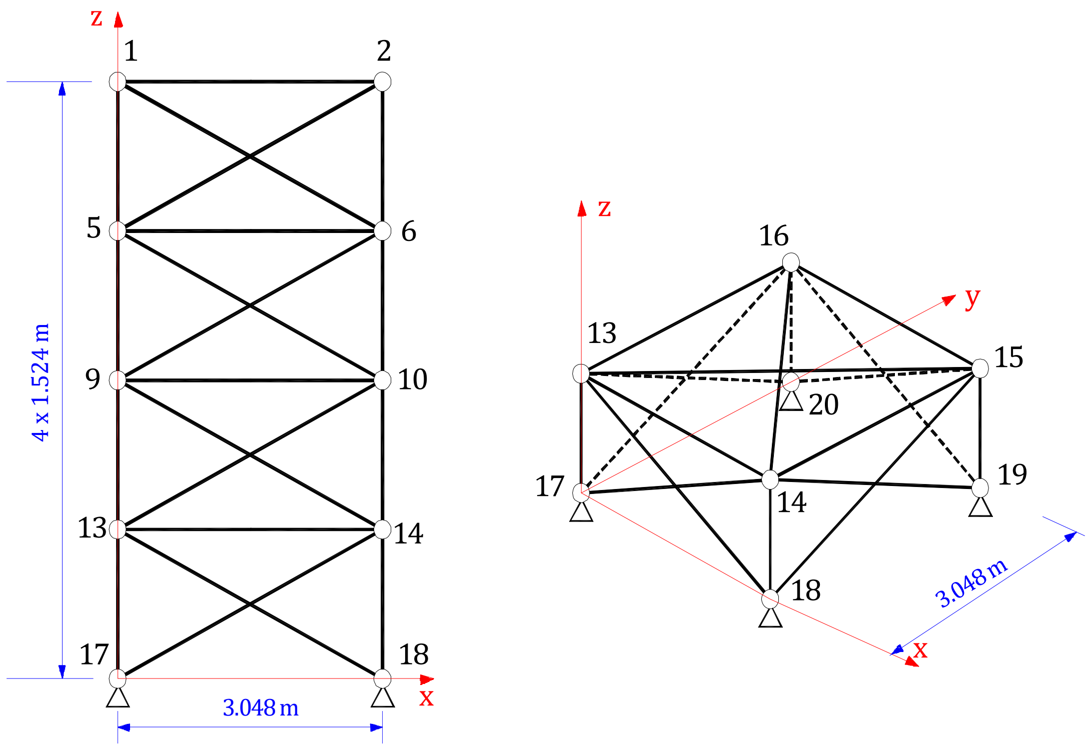

Figure 5: 72-bar truss structure

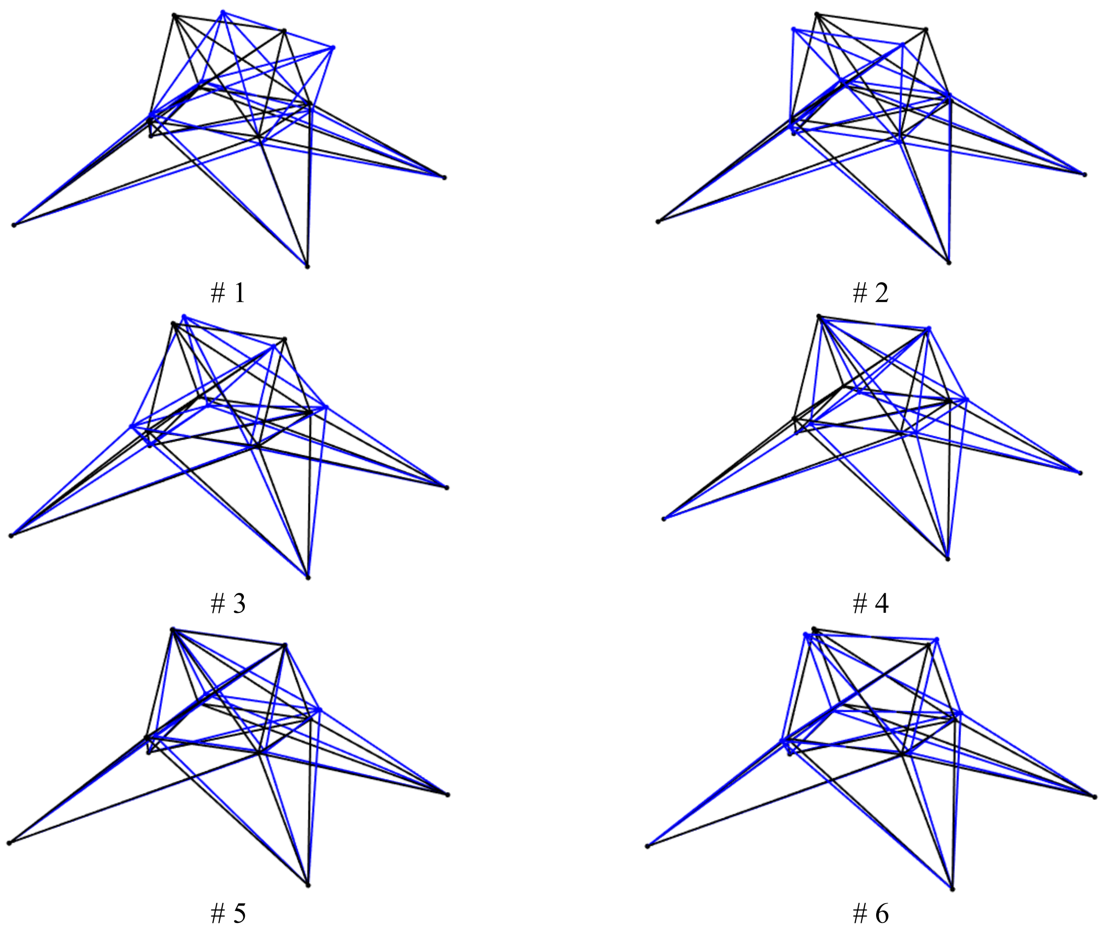

Figure 6: The first six mode shapes of 25-bar truss structure

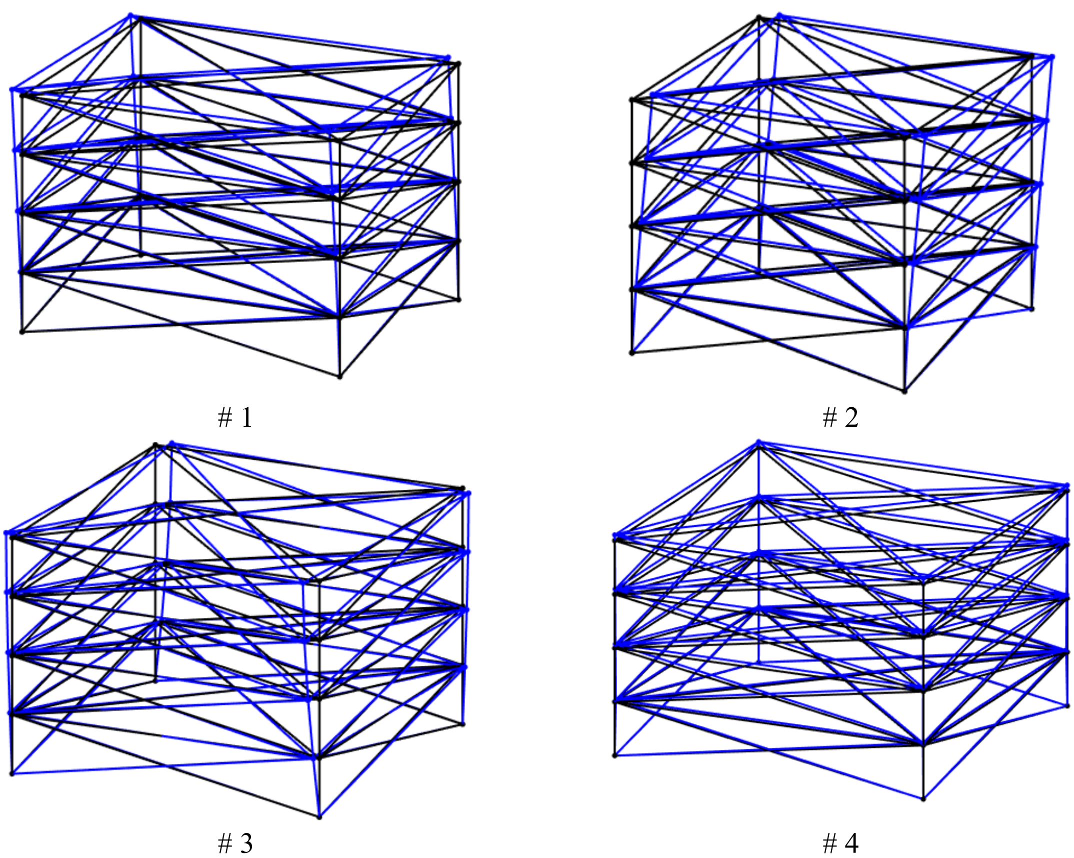

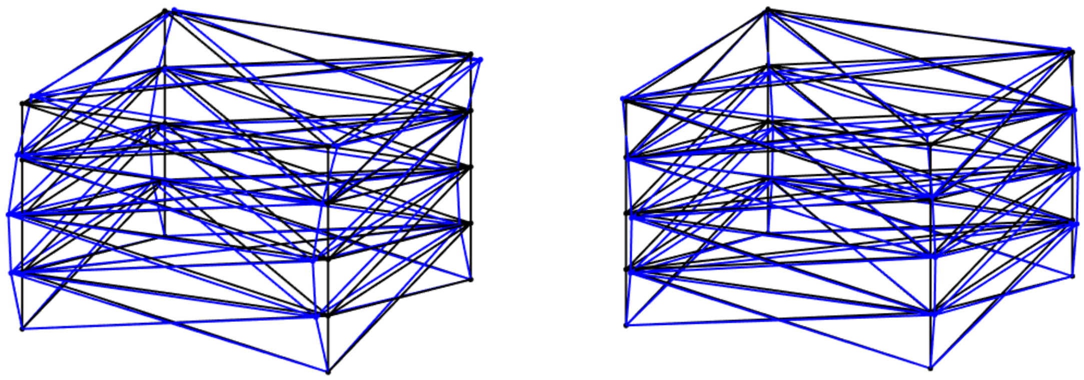

5 # 6

Figure 7: The first six mode shapes of 72-bar truss structure

Table 1: Properties of bar

A	*E*	*ρ*
0.000707 m^2	205e9 N/m^2	7833 kg/m^3

Table 2: Coordinates of nodes

25-bar truss structure				72-bar truss structure							
Node	**x (m)**	**y (m)**	**z (m)**	**Node**	**x (m)**	**y (m)**	**z (m)**	**Node**	**x (m)**	**y (m)**	**z (m)**
1	-0.9525	0	5.08	**1**	0	0	6.096	**11**	3.048	3.048	3.048
2	0.9525	0	5.08	**2**	3.048	0	6.096	**12**	0	3.048	3.048
3	-0.9525	0.9525	2.54	**3**	3.048	3.048	6.096	**13**	0	0	1.524
4	0.9525	0.9525	2.54	**4**	0	3.048	6.096	**14**	3.048	0	1.524
5	0.9525	-0.9525	2.54	**5**	0	0	4.572	**15**	3.048	3.048	1.524
6	-0.9525	-0.9525	2.54	**6**	3.048	0	4.572	**16**	0	3.048	1.524
7	-2.54	2.54	0	**7**	3.048	3.048	4.572	**17**	0	0	0
8	2.54	2.54	0	**8**	0	3.048	4.572	**18**	3.048	0	0
9	2.54	-2.54	0	**9**	0	0	3.048	**19**	3.048	3.048	0
10	-2.54	-2.54	0	**10**	3.048	0	3.048	**20**	0	3.048	0

Table 3: Two nodes of each bars

25-bar truss structure			72-bar truss structure								
Bar	**Nodes**		**Bar**	**Nodes**		**Bar**	**Nodes**		**Bar**	**Nodes**	
1	1	2	**1**	1	5	**26**	6	11	**51**	11	12
2	1	4	**2**	2	6	**27**	8	12	**52**	9	12
3	2	3	**3**	3	7	**28**	7	12	**53**	9	11
4	1	5	**4**	4	8	**29**	8	9	**54**	10	12
5	2	6	**5**	1	6	**30**	5	12	**55**	13	17
6	2	4	**6**	2	5	**31**	5	6	**56**	14	18
7	2	5	**7**	3	6	**32**	6	7	**57**	15	19
8	1	3	**8**	2	7	**33**	7	8	**58**	16	20
9	1	6	**9**	4	7	**34**	5	8	**59**	13	18
10	3	6	**10**	3	8	**35**	5	7	**60**	14	17
11	4	5	**11**	4	5	**36**	6	8	**61**	15	18
12	3	4	**12**	1	8	**37**	9	13	**62**	14	19
13	5	6	**13**	1	2	**38**	10	14	**63**	16	19
14	3	10	**14**	2	3	**39**	11	15	**64**	15	20
15	6	7	**15**	3	4	**40**	12	16	**65**	16	17
16	4	9	**16**	1	4	**41**	9	14	**66**	13	20
17	5	8	**17**	1	3	**42**	10	13	**67**	13	14
18	4	7	**18**	2	4	**43**	11	14	**68**	14	15
19	3	8	**19**	5	9	**44**	10	15	**69**	15	16
20	5	10	**20**	6	10	**45**	12	15	**70**	13	16

25-bar truss structure			72-bar truss structure								
Bar	**Nodes**		**Bar**	**Nodes**		**Bar**	**Nodes**		**Bar**	**Nodes**	
21	6	9	**21**	7	11	**46**	11	16	**71**	13	15
22	6	10	**22**	8	12	**47**	12	13	**72**	14	16
23	3	7	**23**	5	10	**48**	9	16			
24	4	8	**24**	6	9	**49**	9	10			
25	5	9	**25**	7	10	**50**	10	11			

Natural frequencies and mode shapes are combined to form the objective function (*ob*). Equation (8) must be solved in order to determine these frequencies and mode shapes:

$$[M]\ddot{d}+[K]d=0 \tag{8}$$

from which:

$$d=\xi\sin(\omega t+\varphi) \tag{9}$$

$$\ddot{d}=-\omega^2\xi\sin(\omega t+\varphi) \tag{10}$$

So Equation (8) can be rewritten:

$$\left([K]-\omega^2[M]\right)\xi=0 \tag{11}$$

$$\left\|[K]-\omega^2[M]\right\|=0 \tag{12}$$

Note that:

$$f_i=\omega_i/2\pi \tag{13}$$

The global stiffness matrix K is going to decrease if any member of the truss structure is damaged. With K_e as the stiffness matrix of an element (a member), if it goes down *r*%, K also declines to a certain extent.

$$\mathrm{K}_e^d=(1-r\%)\mathrm{K}_e \tag{14}$$

Table 4: The damage situations of 25-bar truss structure

Situations	Damage bar(s)	Severity of damage
The first situation	Bar 24	40%
The second situation	Bar 3 Bar 25	35% 25%
The third situation	Bar 1 Bar 10 Bar 15	35% 25% 20%
The fourth situation	Bar 1 Bar 4 Bar 10 Bar 15	35% 30% 25% 20%

Then the objective function is depicted by Equation (15):

$$ob=\zeta_1\sqrt{\sum_{i=1}^{6}\frac{\left(f_i^c-f_i^m\right)^2}{\left(f_i^m\right)^2}}+\zeta_2\left(1-\frac{\left(\left|\sum_{i=1}^{6}\xi_i^c\xi_i^m\right|\right)^2}{\left(\sum_{i=1}^{6}\left(\xi_i^c\right)^2\right)\left(\sum_{i=1}^{6}\left(\xi_i^m\right)^2\right)}\right) \tag{15}$$

With 6 being the number of considered natural frequencies and mode shapes, (*m*) and (*c*) indicate the "*measured*" and "*computed*", f_i and ξ_i are the *i*th natural frequency and mode shape. Figures 6 & 7 depict the first six mode shapes of 25-bar and 72-bar space truss structures.

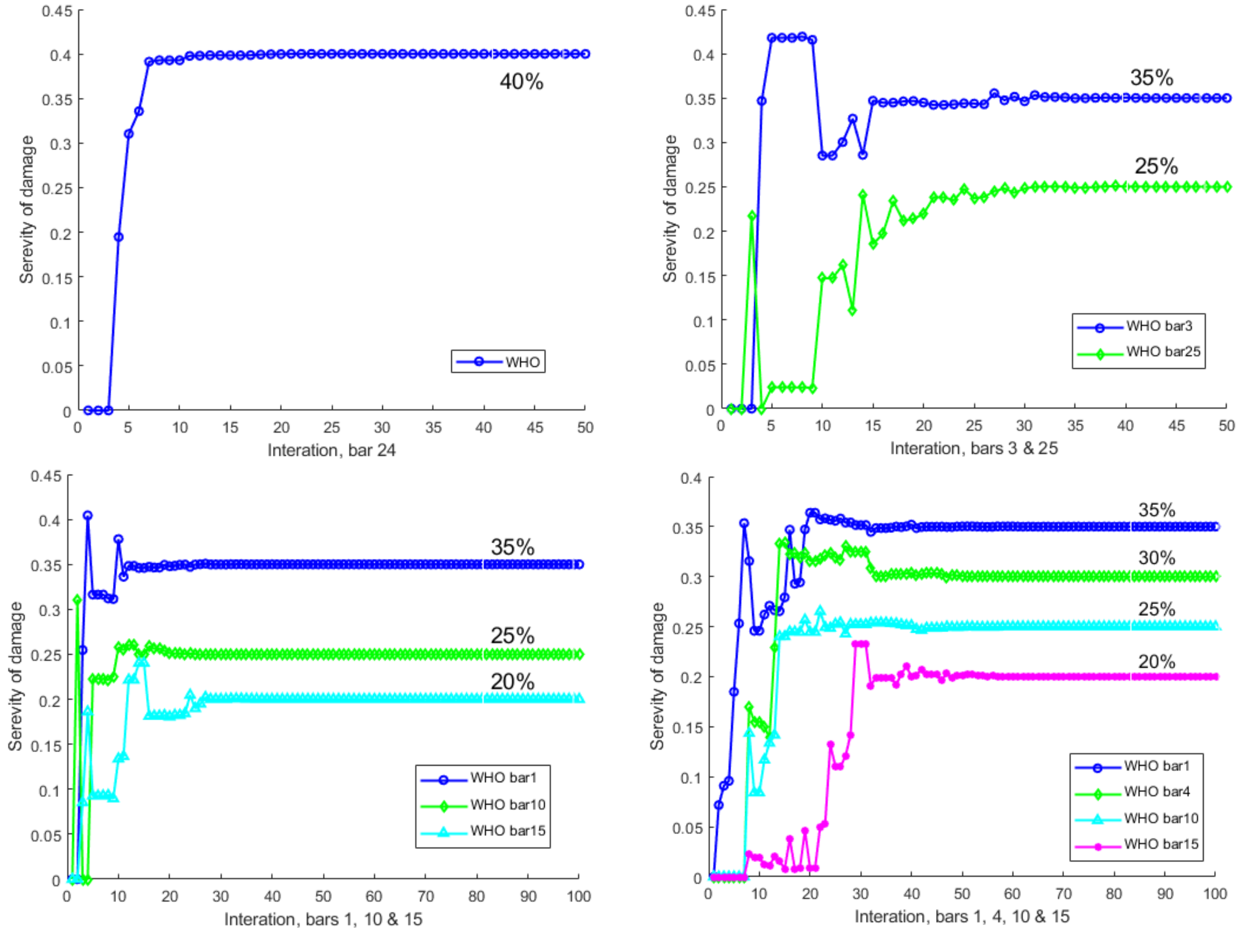

Figure 8*:* The convergence for the damage situations of 25-bar truss structure

Table 5: The damage situations of 72-bar truss structure

Situations	Damage bar(s)	Severity of damage
The first situation	Bar 13	40%
The second situation	Bar 4 Bar 22	35% 25%
The third situation	Bar 25 Bar 41 Bar 69	35% 25% 20%
The fourth situation	Bar 1 Bar 25 Bar 41 Bar 67	40% 35% 25% 20%

To confirm the correctness, certain damage situations are shown in Tables 4 and 5. The results, which are shown in Figures 8 to 9, demonstrate that the WHO produces the anticipated results for damage structure prediction. Furthermore, it is clear that the WHO only needs roughly 100 iterations to produce the necessary results.

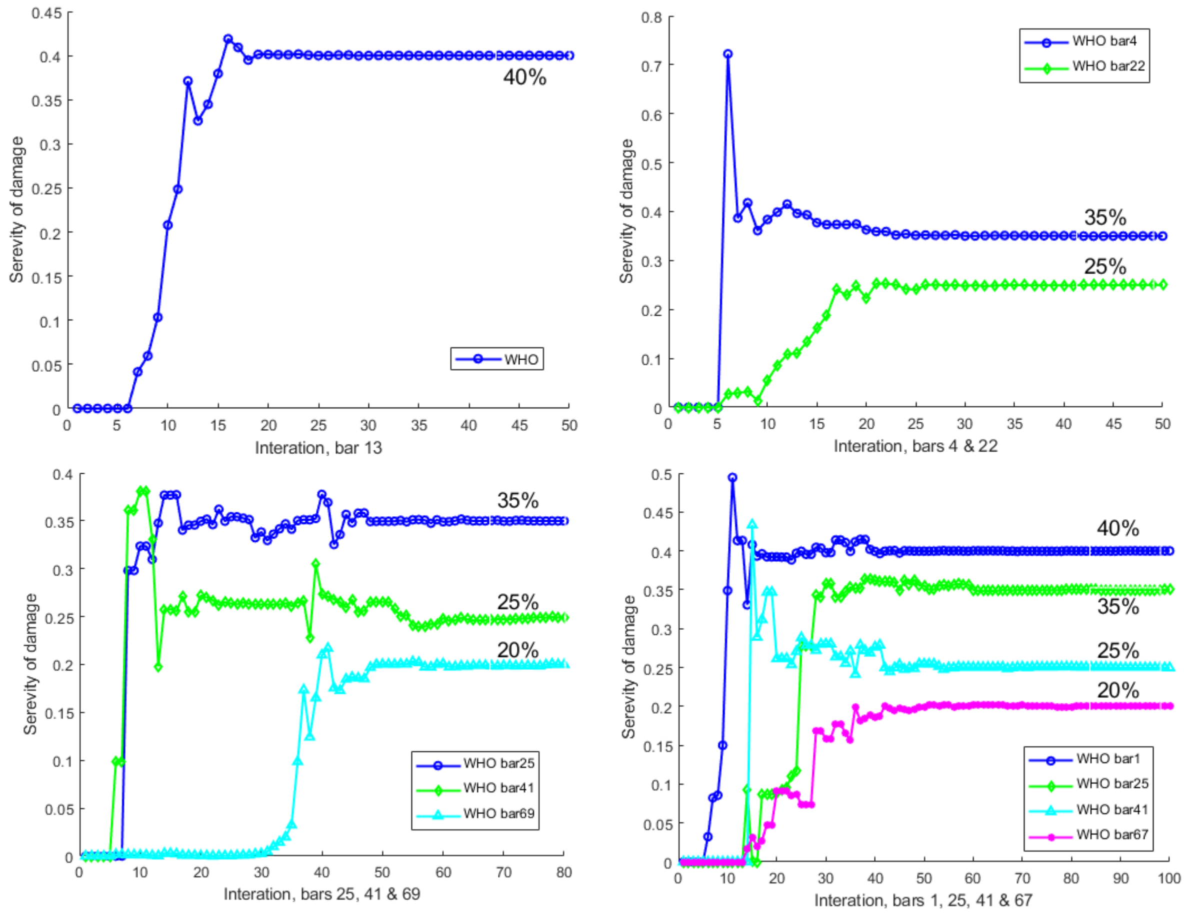

Figure 9: The convergence for the damage situations of 72-bar truss structure

4. CONCLUSION

This paper shows how to utilize the Wild Horse Optimizer (WHO) to identify damage in space truss structures. The algorithm's performance is assessed in a variety of situations, ranging from straightforward to intricate, and the results show how effectively the WHO predicts the position and magnitude of damage.

DECLARATION OF CONFLICTING INTERESTS

The author declares no potential conflicts of interest with respect to the research and publication of this paper.

REFERENCES

[1] R. Poli, J. Kennedy, and T. Blackwell, "Particle swarm optimization," Swarm Intelligence, Vol. 1, pp. 33–57, https://doi.org/10.1007/s11721-007-0002-0, (2007)

[2] R. Cazacu and L. Grama, "Steel truss optimization using genetic algorithms and FEA," Procedia Technology, Vol. 12, pp. 339–346, https://doi.org/10.1016/j.protcy.2013.12.496, (2014)

[3] E. Rashedi, H. Nezamabadi-pour, and S. Saryazdi, "GSA: A gravitational search algorithm," Information Sciences, Vol. 179(13), pp. 2232–2248, https://doi.org/10.1016/j.ins.2009.03.004, (2009)

[4] S. Mirjalili, A. H. Gandomi, S. Z. Mirjalili, S. Saremi, H. Faris, and S. M. Mirjalili, "Salp swarm algorithm: A bio-inspired optimizer for engineering design problems," Advances in Engineering Software, Vol. 114, pp. 163–191, https://doi.org/10.1016/j.advengsoft.2017.07.002, (2017)

[5] D. Karaboga and B. Basturk, "A powerful and efficient algorithm for numerical function optimization: Artificial bee colony (ABC) algorithm," Journal of Global Optimization, Vol. 39, pp. 459–471, https://doi.org/10.1007/s10898-007-9149-x, (2007)

[6] S. Mirjalili, S. M. Mirjalili, and A. Lewis, "Grey wolf optimizer," Advances in Engineering Software, Vol. 69, pp. 46–61, https://doi.org/10.1016/j.advengsoft.2013.12.007, (2014)

[7] I. Naruei and F. Keynia, "Wild horse optimizer: A new meta-heuristic algorithm for solving engineering optimization problems," Engineering with Computers, Vol. 38, pp. 3025–3056, https://doi.org/10.1007/s00366-021-01438-z, (2022)

[8] H.-G. Beyer and H.-P. Schwefel, "Evolution strategies-A comprehensive introduction," Natural Computing, Vol. 1, pp. 3–52, https://doi.org/10.1023/A:1015059928466, (2002)

[9] K. Luo, "Water flow optimizer: A nature-inspired evolutionary algorithm for global optimization," IEEE Transactions on Cybernetics, Vol. 52(8), pp. 7753–7764, https://doi.org/10.1109/TCYB.2021.3049607, (2022)

[10] S. Mirjalili, "SCA: A sine cosine algorithm for solving optimization problems," Knowledge-Based Systems, Vol. 96, pp. 120–133, https://doi.org/10.1016/j.knosys.2015.12.022, (2016)

[11] V. Hayyolalam and A. A. P. Kazem, "Black widow optimization algorithm: A novel meta-heuristic approach for solving engineering optimization problems," Engineering Applications of Artificial Intelligence, Vol. 87, p. 103249, https://doi.org/10.1016/j.engappai.2019.103249, (2020)

[12] R. V. Rao, V. J. Savsani, and D. P. Vakharia, "Teaching–learning-based optimization: A novel method for constrained mechanical design optimization problems," Computer-Aided Design, Vol. 43(3), pp. 303–315, https://doi.org/10.1016/j.cad.2010.12.015, (2011)

[13] S. Talatahari and M. Azizi, "Chaos game optimization: A novel metaheuristic algorithm," Artificial Intelligence Review, Vol. 54, pp. 917–1004, https://doi.org/10.1007/s10462-020-09867-w, (2021)

[14] H. L. Ton-That, "Natural frequencies of functionally graded sandwich plates resting on an elastic foundation using Chebyshev finite element method," Acta Mechanica et Automatica, Vol. 19(2), pp. 318–326, https://doi.org/10.2478/ama-2025-0039, (2025)

[15] H. L. Ton-That, "Analysis of natural frequency of porous sigmoid functionally graded sandwich plates via another quadrilateral element," Journal of Theoretical and Applied Mechanics, Vol. 55(2), pp. 188–201, https://doi.org/10.55787/jtams.25.55.2.188, (2025)